

# Seepage Shear Failure of Sandy Soils by Pore Water Injection Test

Kazama M, Uzuoka R, Sento N, Unno T

(Dept. of Civil Engineering, Tohoku University, Sendai, 980-8579, Japan)

**Abstract:** The possibility of a flow failure due to seepage with the redistribution of the excess pore water pressure after liquefaction has been pointed out. To study this phenomenon, the seepage shear failure of the soils subjected to pore water injection is examined by laboratory tri-axial test. In the test, after anisotropic consolidation, keeping the deviator stress, pore water is injected using pore water control apparatus under a constant volumetric strain controlled condition. The materials used in the tests are ordinary fine clean sand and the weathered granite soil, which liquefied during the 1995 Kobe earthquake. Based on the test results, the seepage shear failure criteria due to pore water injection and the shear strain development characteristics regarding a post-liquefaction behavior are discussed.

**Key word:** Seepage shear failure; Weathered granite soil; Post-liquefaction; Pore water injection

## 沙土在孔隙水注入实验中渗透剪切破坏

Kazama M, Uzuoka R, Sento N, Unno T

(东北大学土木工程系, 仙台 980-8579, 日本)

**摘要:**前人曾指出液化后伴随着超孔隙水压重新分配的渗透会引起流体破坏的可能性。为了研究这一现象,利用实验室三轴试验将孔隙水注入土壤检测了土壤的渗透剪切破坏。该实验是在各项异性的固结作用后保持差应力,使用孔隙水控制装置在体积不变的应变控制条件下将孔隙水注入。实验中所用的材料是在 1995 年神户地震时被液化的常规洁净细砂和风化的花岗岩土壤。本文以实验结果为基础,讨论了由孔隙水注入引起的渗透剪切破坏判据和导致后液化行为的剪切应变发展特征。

**关键词:**渗透剪切破坏; 风化花岗岩土壤; 后液化作用; 孔隙水注入

中图分类号: P315.3

文献标识码: A

文章编号: 1000-0844(2005)03-0212-08

## 0 Introduction

Pore water inflow leads sometimes reducing the effective stress condition of a sandy ground, and it causes a shear failure of ground. Hydraulic fracturing of dams, rainfall infiltration of slopes and seepage failure caused by upward pore water flow after liquefactions are the typical examples. In such phenomenon, shear strain develops immediately after the stress state reaches the failure stress condition and it is regarded as a seepage

shear failure induced by pore water inflow. For evaluating the seepage shear failure and the following residual deformation, the strain development characteristic of sandy soil is a key issue. In this paper, the authors focus on the seepage failure after liquefaction and studied the soil deformation property of sandy soils subjected to pore water inflow using sandy soils including the weathered granite soil which liquefied during the 1995 Kobe earthquake.

# 1 Seepage failure caused by liquefaction after earthquake

## 1.1 Outline of the seepage failure mechanism [1-2]

Fig. 1 shows a simple example of three soil layers in order to describe the flow deformation mechanism. The soil profile consists of a silty soil layer with relatively low permeability above a sandy soil layer under the sea floor. Supposing that excess pore water pressure is generated in the respective sandy layers during an earthquake, pore water pressure redistributes the following ways.

(1) Pore pressure in lower layers is much higher than that in the upper layer at the end of an earthquake ( $t_0$ ). (2) Excess pore water pressure in the upper sand layer rises until the initial effective overburden pressure is matched ( $t_1$ ) because pore water is trapped under the silt layer. (3) Upward seepage continues to flow until  $t_2$ , when the excess pore water pressure gradient becomes zero beneath the silt layer. (4) The silt layer continues to consolidate until excess pore water pressure dissipates in all layers.

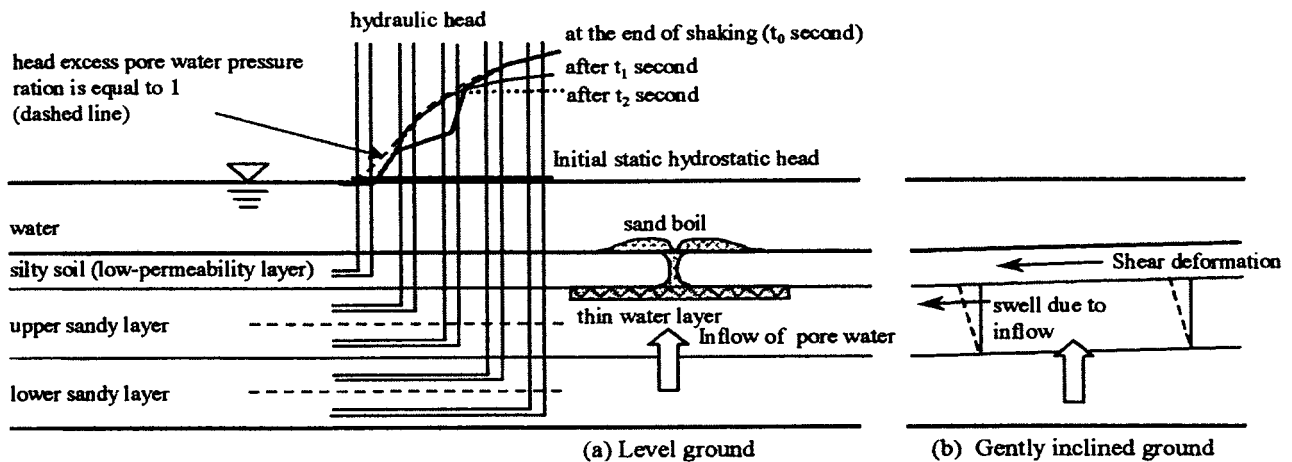


Fig. 1 Schematic diagram of the flow failure mechanism of ground with non-homogeneous soil conditions.

For level ground (like that illustrated in the middle of Fig. 1), if no sand boil occurs due to ground-breaks within the silt layer, soil particle sedimentation occurs and a thin water layer may appear at the silt-sand layer boundary during processes (3) and (4) [3]. In contrast, no matter how slightly the layer is inclined (as illustrated on the right hand side of Fig. 1), gravity subjects the soil layers to constant shear stress. Therefore, when upper sand loses its shear strength due to upward seepage in process (1) to (3), shear strain gradually develops because the upper sand swells and loosens during the period from  $t_1$  to  $t_2$ , while the soil maintains constant shear stress, soil behaves as a solid, not as a fluid. This represents the post-liquefaction flow failure scenario that the authors had proposed [1-2]. In this scenario, it is essential to elucidate the shear strain development characteristics of sand when subjected to shear stress due to gravity in processes (2) and (3).

## 1.2 Stress path of the upper layer

Next, we consider the detailed stress state and volume change behavior of soil elements during the above-mentioned process. Schematic diagrams of stress paths and the related development of volumetric and shear strain are shown in Fig. 2. Diagram corresponds to behavior of the upper sand layer shown in Fig. 1. In this layer pore water inflow from the lower layer occurs subsequent to undrained cyclic shear. In the case of the layer experiencing pore water flow, it is divided into three periods. Section B→C represents the excess pore water pressure increase by inflow. This section corresponds to the period from  $t_0$  to  $t_1$  in Fig. 1. Point C, located on the failure line, shows the threshold state from which shear strain suddenly increases. Section C→C' represents the process in which pore water inflow occurs continuously. This section corresponds to the period from  $t_1$  to  $t_2$  in Fig. 1. In this state, soil elements have already failed

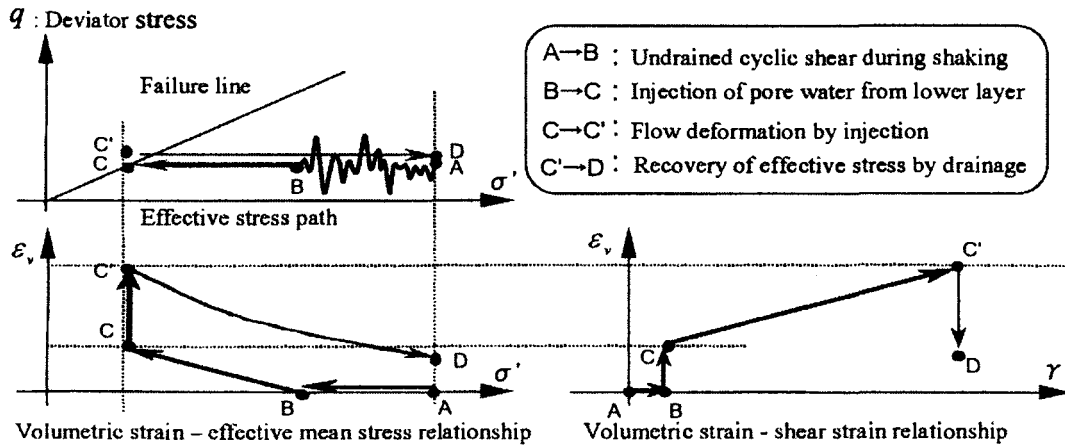


Fig. 2 Schematic diagram of the stress path in the upper layer.

and shear strain develops proportionally to inflow volume. After seepage failure, a re-consolidation of liquefied sand occurs and the stress path returns to the initial condition in section C'→D.

The seepage failure mechanism explained above makes it possible to explain the progressive failure after liquefaction as observed in large earthquakes. However, only a few studies have addressed failure mechanisms like the seepage failure mechanism. Boulanger and Turman<sup>[4]</sup> studied the behavior of sand in the path from A to C' by tri-axial testing. They showed that sand dilates as the excess pore water pressure increases due to pore water injection and further injection renders sand specimens unstable. Tokimatsu et al.<sup>[5]</sup> studied the relation between volumetric and shear strain in the path from C to C' in torsional hollow cylinder test. They revealed that looser sand develops larger shear strain when an equivalent volumetric strain was applied.

## 2 Pore water injection test

### 2.1 Testing materials

The soils used in a laboratory test are two typical sandy soils. One is Toyoura sand as a representative of fine clean sand. The other material is the weathered granite soil, which is well known as the sandy soil liquefied during the 1995 Kobe earthquake. The soil is called Masado and this name is used hereafter. Original Masado soil includes gravelly content about 48% for the under 30

mm<sup>[6]</sup>. In the test, the under 2 mm size grain was used in which fine content of 18% was included. These soils grain-size distributions are plotted in Fig. 3.

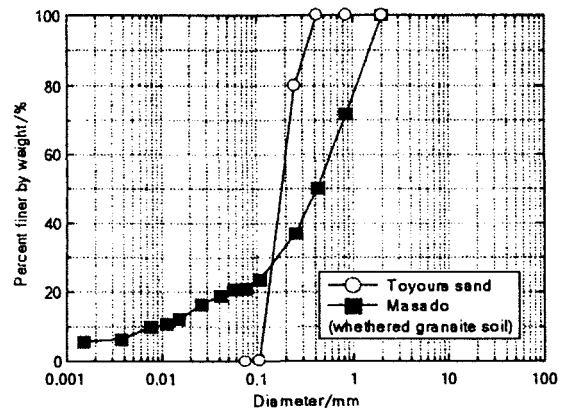


Fig. 3 Grain size distributions.

### 2.2 Testing conditions

Tri-axial test was performed to study the shear failure due to pore water injection. In the test, volumetric strain rates and initial static shear stress were constant and the pore water injection volume was continuously increased until the shear strain develops about 15% to 25%. The volumetric strain control device used is shown in Fig. 4. The device is based on the concept of DPVC (Digital Pressure/Volume Controller)<sup>[7]</sup>, and its theoretical resolution of volumetric strain is  $1.27 \times 10^{-5} \%$  /pulse. Sample dimensions are 50 mm in diameter and 100 mm in height. Constant initial static shear stress was applied by air pressure through pneumatic loader.

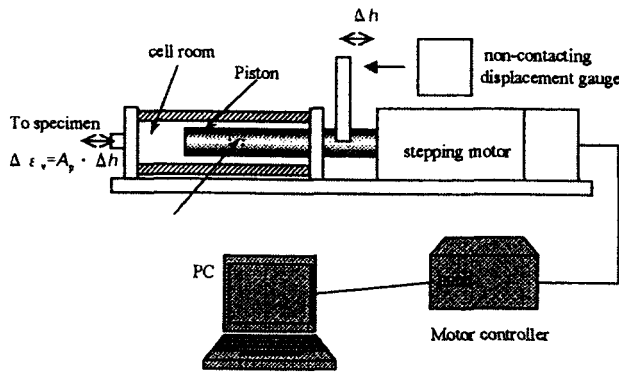


Fig. 4 Volumetric strain control device.

Specimens were prepared by the air-pluviation method for Toyoura sand and had relative densities of ( $D_r$ ) 40%, 60% and 90%. On the other hand, specimens of Masado soil were prepared by compaction with mallet before consolidation, because it was reported that density control is difficult for Masado due to its collapsible nature during a consolidation and a saturation<sup>[8-9]</sup>.

Fig. 5 shows the stress path of the tests. Two types of tests were performed; a V-CST test (Volume strain controlled, Constant Shear Tri-axial test) and CD test (Consolidated Drained tri-axial test) for normally consolidated specimens. In V-CST test, the volume strain rate was 0.04%/min. in the CD test, the shear strain rate was 0.1%/min. Axial strain and pore pressure were measured during the test under volume strain and deviator stress controlled condition.

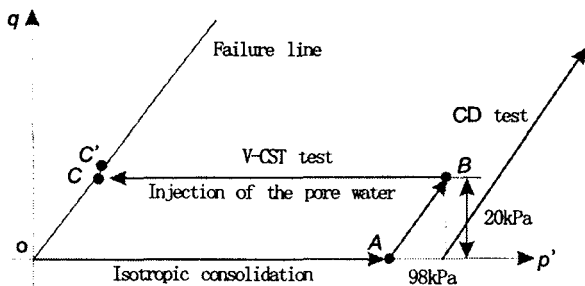


Fig. 5 Stress path of the V-CST test and CD test.

### 3 Test result

#### 3.1 Definition of seepage failure of V-CST tests

Fig. 6 shows the typical test results obtained from V-CST tests. These figures shows the relationship of  $p' \rightarrow q, \epsilon_v \rightarrow \gamma$  and  $\epsilon_v \rightarrow p'$ , where  $\epsilon_v =$  the volumetric strain and  $\gamma =$  the shear strain. Based

on the test results, three typical states were observed during the tests as described in Fig. 6; (I) Elastic state; in this state, an elastic behavior is dominant and the developed shear strain is small. (II) Unstable pre-failure state; before the stress state reaches the failure line, there is the point from where the large shear strain development starts. In Fig. 6, the point is named an Initial Yielding Point (IYP). This region is especially clear for loose sand as shown in later. (III) Seepage failure state; the state after the stress state reaches the failure line in the  $p' \rightarrow q$  plane. In this state, the ratio of  $d\epsilon_v/d\gamma$  becomes almost constant, where  $d\epsilon_v$  and  $d\gamma$  denote the increment of volumetric and shear strain. Even after the sample reaches the initial seepage failure line, the behavior was observed that the effective mean stress decreases gradually. In Fig. 6 the Seepage Failure Point represents (SFP). In the following section, the authors pay attention to these two points IYP and SFP.

#### 3.2 Relationship between the shear and volumetric strain

Fig. 7 shows the relationship between the shear and volumetric strain obtained. Figure 7(b) is the magnified one in small shear strain region of figure 7(a). Large shear strains develop after the samples reach the IYP, with volumetric strains from about 0.2% to 0.5%. Looser Toyoura sand develops larger shear strains when equivalent volumetric strains are applied. This indicates that denser sand has high resistance against seepage failure. For Masado with relative density  $D_r = 90\%$ , the incremental strain ratio ( $d\epsilon_v/d\gamma$ ) is almost the same as that obtained for Toyoura sand. Unstable pre-failure state, which is the condition between IYP and SFP, is much clear for the sand with smaller relative density. This represents that the fabric change starts before the failure stress state for loose sand.

#### 3.3 Relationship between the volumetric strain and the effective mean stress

Fig. 8 shows the relationship between the volumetric strain and the effective mean stress obtain

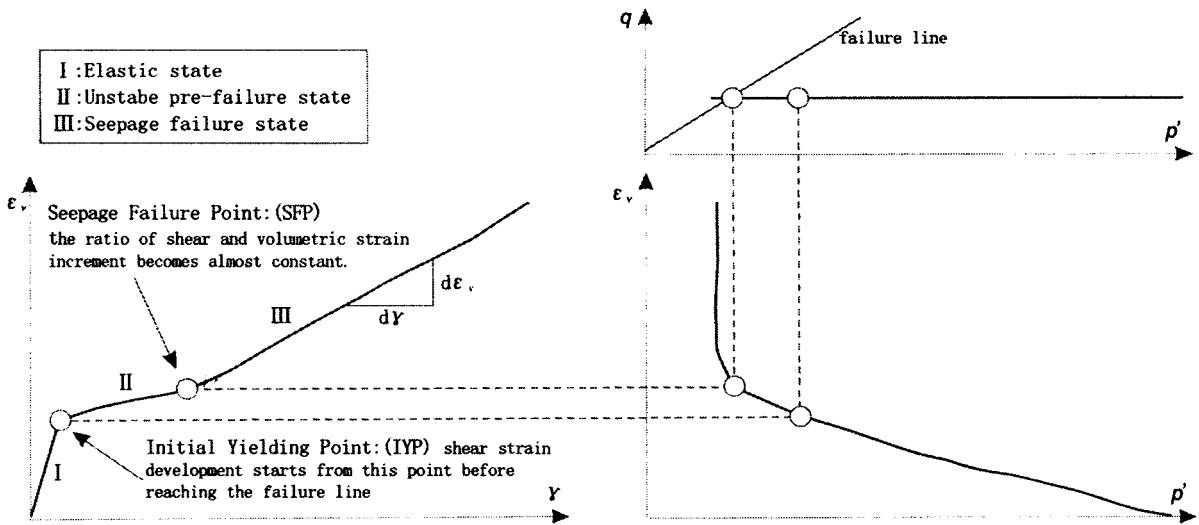


Fig. 6 Schematic diagram of the typical relationship observed in a pore water injection test (V-CST test).

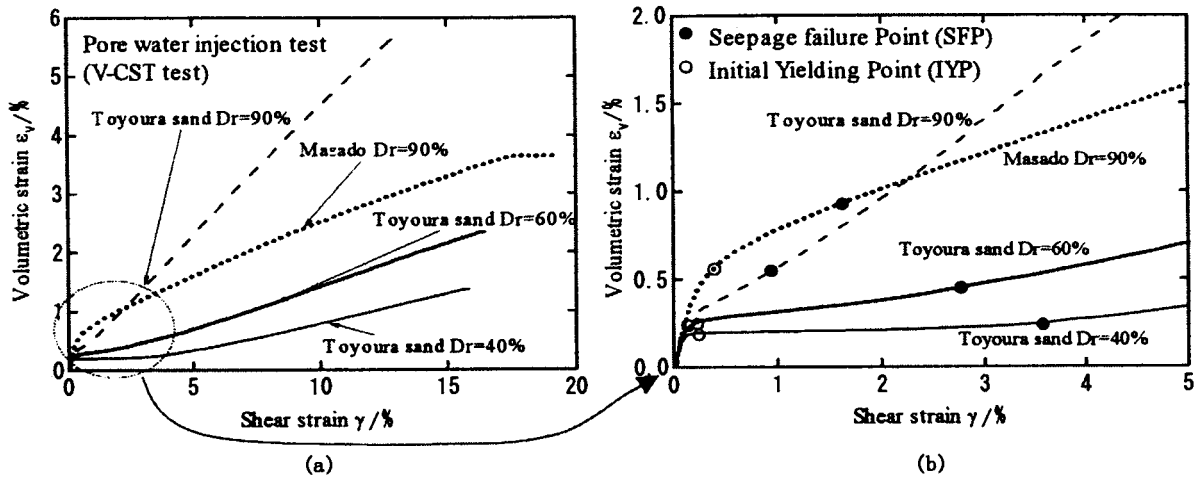


Fig. 7 Relationship between the shear and volumetric strain obtained from V-CST test.

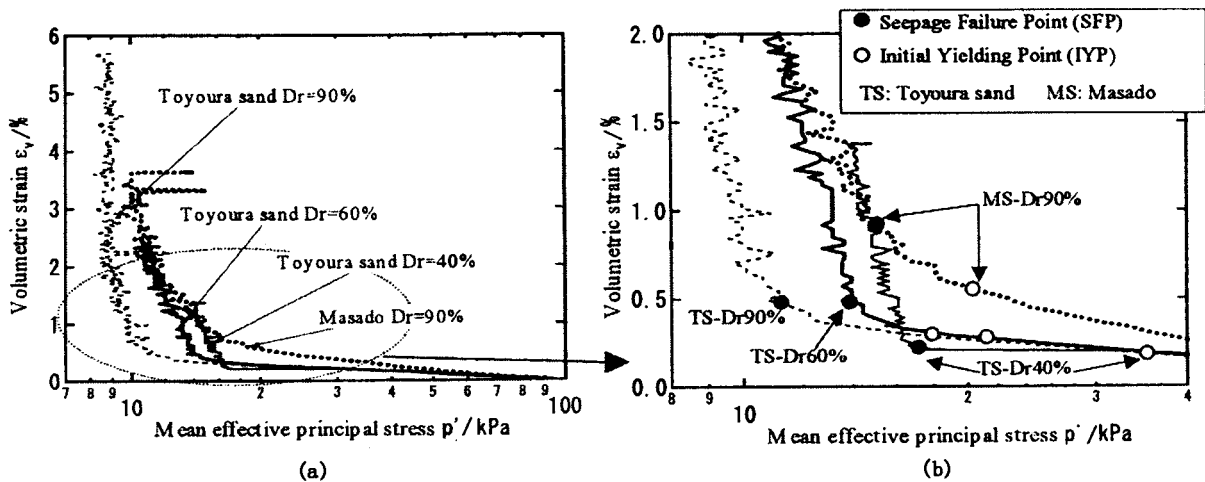


Fig. 8 Relationship between the volumetric strain and the effective mean stress obtained from V-CST tests.

ed from V-CST test. Figure 8(b) is the magnified one in the small volumetric strain region of figure 8(a). Denser Toyoura sand reaches the seepage

failure point (SFP) at smaller effective mean stress. This indicates that denser sand has large frictional angle against seepage. For Masado, the

effective mean stress at SFP is almost the same as that obtained for Toyoura sand with relative density  $D_r = 60\%$ . After the specimens reach the failure line, the effective mean stress decreases gradually with small vibration. This represents that the fabric change occurred for mobilizing the constant shear stress under the volume change condition.

### 3.4 Comparison of $\epsilon_v - \gamma$ relationship with that of CD tests

Fig. 9 shows the relationship between volumetric and shear strain obtained from the Consolidated and Drained tri-axial test (CD test). For sand with same relative density, the positive dilat-

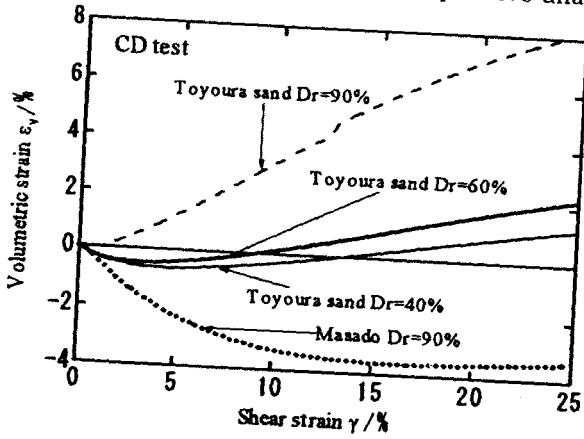


Fig. 9 Relationship between volumetric and shear strain.

Fig. 11 shows the relation between the stress ratio and shear strain both from the CD test and V-CST test for Masado soil and Toyoura sand with relative density 60%. For Toyoura sand, the relation obtained from the CD test is well consistent with that obtained from the V-CST test. For Masado soil, the stress ratio mobilized at the same strain level in the CD test is smaller than that of the V-CST test more significantly. These results support the difference of the  $d\epsilon_v/d\gamma$  at SFP described before. It is considered that the soil with low water content like Masado soil demonstrates shear resistance gradually in the drained compression shear of the CD test. This may be dependent on the difference of the confining stress level at the failure state between the CD test and the V-CST test. According to this result, it can be concluded that Masado has much stronger resistance to the

seepage failure in low confining pressure condition than compression shear failure in relative high confining stress condition. Fig. 12 shows the relationship between the deviator stress ratio  $q/p'$  and the strain increment ratio  $d\epsilon_v/d\gamma$  obtained from both the V-CST and the CD test. For Toyoura sand the relation reaches steady point for two tests. On the other hand, for Masado soil the final relation does not match for two tests.

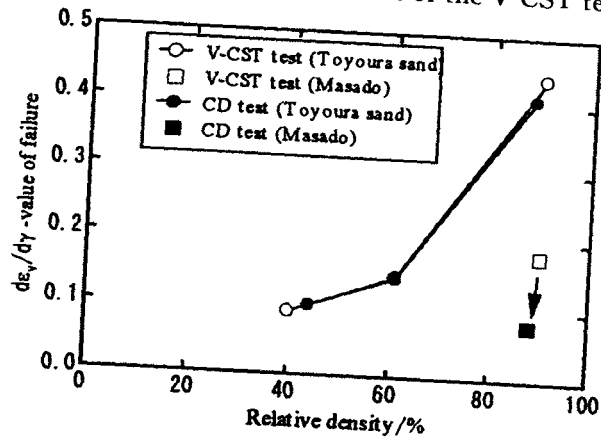


Fig. 10 Comparison of  $(d\epsilon_v/d\gamma)$  at failure state.

seepage failure in low confining pressure condition than compression shear failure in relative high confining stress condition.

Fig. 12 shows the relationship between the deviator stress ratio  $q/p'$  and the strain increment ratio  $d\epsilon_v/d\gamma$  obtained from both the V-CST and the CD test. For Toyoura sand the relation reaches steady point for two tests. On the other hand, for Masado soil the final relation does not match for two tests.

## 4 Conclusions and remarks

Seepage shear failure of sand soils was studied by pore water injection test using a tri-axial test, the following results were obtained from this study:

- (1) During the pore water injection in keeping a constant deviator stress, three typical soil states

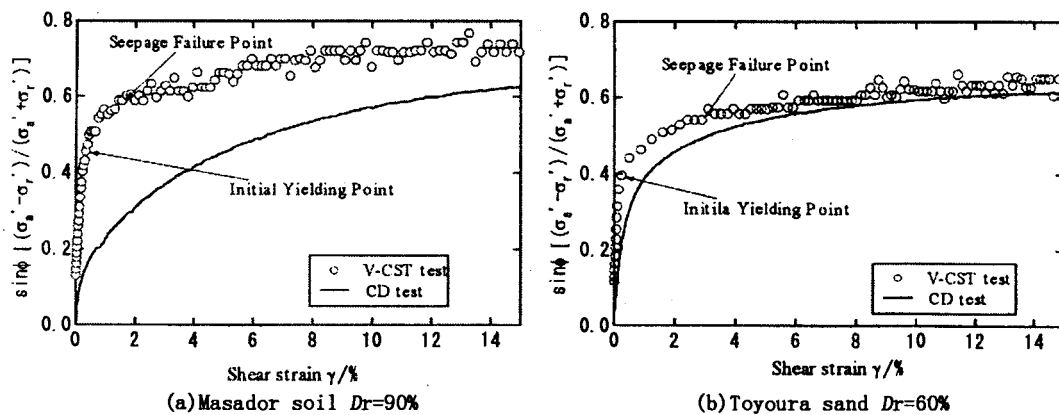


Fig. 11 Comparison of the stress ratio and shear strain relationship for Masador soil and Toyoura sand.

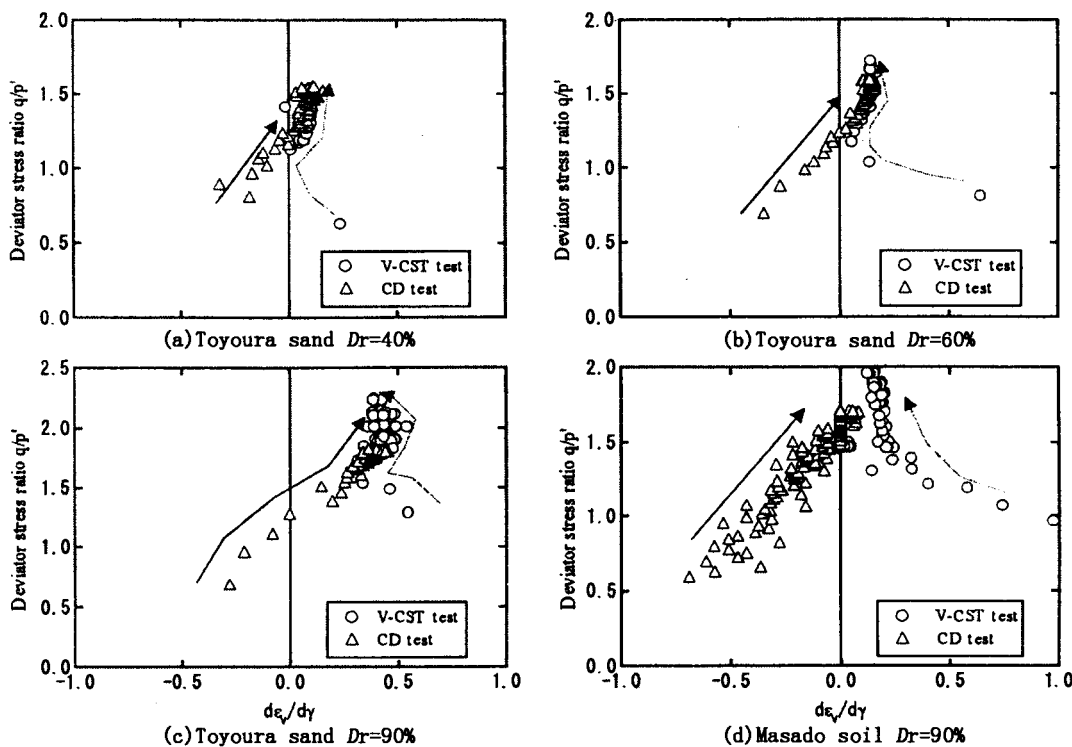


Fig. 12 Relationship between the deviator stress ratio  $q / p'$  and the strain increment ratio  $d\varepsilon_x / d\gamma$ .

were observed: I ) Elastic state, II ) Unstable pre-failure state and III ) Seepage failure state. These states were divided by Initial Yielding Point (IYP) and Seepage Failure Point (SFP).

(2) After the soils reach the IYP, the shear strain develops almost in proportion to injected pore water volume. To develop the same shear strain level, denser sand requires much more injected pore water.

(3) For Toyoura sand as a representative of fine clean sand, the ratio of the shear and the vol-

umetric strain in seepage failure state is consistent with that obtained from the CD-test. This indicates that shear strain development behavior under constant volume injection are considered to be governed by dilatancy characteristics of sand.

(4) However, for Masador soil which is the weathered granite soil liquefied during the 1995 Kobe earthquake, the ratio of the shear and the volumetric strain in the pore water injection test is much larger than that obtained from the CD-test. Masador soil has much stronger resistance to the seepage failure in low confining pressure condition

than compression shear failure in relative high confining stress condition. This may be caused by the fine content or collapsible particle nature. Further study will be necessary for this point.

#### [Reference]

- [1] Sento N, Ohmura H, Akahori K, et al. New prediction Method for Ground Flow Deformation due to Seepage after Earthquake[J]. *Tsuchi-To-Kiso*, 2002, **50**(2): 13—15 (in Japanese).
- [2] Sento N, Kazama M, Uzuoka R, et al. Possibility of post-liquefaction flow failure due to seepage[J]. *Journal of Geotechnical and Geo-environmental Engineering*, ASCE, 2004, ( to be appeared).
- [3] Kokusho T. Water film in liquefied sand and its effect on lateral spread[J]. *Journal of Geotechnical and Geo-environmental Engineering*, ASCE, 1999, **125**(10):817—826.
- [4] Boulanger R W, Turman S P. Void redistribution in sand under post earthquake loading[J]. *Canadian Geotechnical Journal*, 1966, **33**:829—324.
- [5] Tokimatsu K, Taya Y, Zhang J M. Effects of pore water redistribution on post-liquefaction deformation of sands[A]. in: *Proc. , 15th Int. Conf. On Soil Mechanics and Geotechnical Engineering*[C]. Turkey, 2001. 289—292.
- [6] Kazama M, Sento N, Omura H, et al. Liquefaction and Settlement of Reclaimed Ground with Gravelly Decomposed Granite Soil[J]. *Soils and Foundations*, 2003, **43**(3): 57—72.
- [7] Uchida K, Vaid Y P. Sand behavior under strain path control [A]. in: *Proceedings of the 8th International Conference on Soil Mechanics and Geotechnical Engineering* [C]. India, 1994. 17—20.
- [8] Fukuda M, Nakazawa J. Subsidence of Embankment due to Submergence and its Estimation — With Special Reference to Weathering Sandy Soil like Decomposed Granite Soil[J]. *Soil and Foundations*, 1977, **17**(2): 65—73.
- [9] Kazama M, Kagatani T, Yanagisawa E. Peculiarities of liquefaction resistance of Masado[J]. *Journal of Geotechnical Engineering*, JSCE, 2000, **645**, 153—166. (in Japanese).